Journal Media and Communication Studies Vol. 1(6)pp. 106-115, December, 2009
Available online http://www.academicjournals.org/jmcs

Full Length Research Paper

Recent applications of the electrooptic modulators in radio-over-fiber (ROF)

Abd El-Naser A. Mohammed*, M. A. Metawe'e, Abd El-Fattah A. Saad and Mohammed S. F. Tabbour

Department of Electronic and Electrical Communication Engineering, Faculty of Electronic Engineering, Menouf, 32951, Egypt.

Accepted 13 November, 2009

Design of electrooptic modulators in the applications of radio-over-fiber (ROF) has been studied and investigated in the present paper. Integrated optic design is handled to build a tank circuit to obtain the maximum output power. The modulated bandwidth is deeply and parametrically studied over wide ranges of the affecting sets of parameters via specially designed software which processes the interaction of causes and effects. The design parameters of the tank circuit have been processed over large operating requirements. The output due to the nonlinear distortion has been also analyzed, and its penalty is computed. Crystal modulator made of Potassium Dihydrogen Phosphate (KDP) crystal is processed.

Key words: Electrooptic modulators, radio over fiber, design.

INTRODUCTION

Radio-Over-Fiber (ROF) technology enables the transmission of radio signals directly over optical fiber, addressing increasing capacity demands and limited optical network coverage (Chul et al., 2009; Pirelli Broadband Solution, 2006). Radio – over – fiber technology and applications have been recently built up over wide ranges. This technique has succeeded to engage both the fields of radio and optical communication systems. A system based on this technology has been suggested as a cost effective solution to meet modern ever increasing user bandwidth demands and mobility in optical networks (Kim et al., 2003). Radio over fiber has enormous potential for future broadband wireless applications.

High-speed optical modulators are the key components in optical communications and have been widely used in many commercial and military applications, although most of the high-speed electrooptic modulators reported have been fabricated in lithium niobate GaAs, or InP, more recently, polymer-based modulators also have been showing a greater promise. Polymers were emerging as new and interesting materials for optical devices, and such optical waveguides have attracted a considerable attention for their possible applications as optical components in the optical communication systems. The key requirements for optical waveguide materials include a simple and straightforward fabrication process, low optical loss, high-thermal stability, and easy control of refractive index. Low-cost components for the next generation of metro and optical access systems are needed, and here, the polymer devices have a real edge over competing technologies. Recently, the electrooptic polymers have attracted an extensive attention as the materials with which to build modulators because of their advantages over inorganic materials. Such advantages are due mainly to the low dielectric constant of the polymer, the low dispersion between the infrared, and the millimeter-wave frequencies, the excellent velocity match between the carrier optical wave and the modulating microwaves, the large electrooptic coefficient, and the fast electronic response (Azizur et al., 2006).

The high-speed spot communication with the ROF technology was introduced for intelligent transport systems application. A 60-GHz point-to-multipoint wireless access link with a transceiver module and fiber-optic-millimeter-wave transmission was developed. A full-duplex 60-GHz-band millimeter-wave radio-on-fiber system using a single light source was reported (Chang et al., 2007).

In radio over fiber (ROF) systems, two subcarrier modulations (SCMs), that is, single-sideband (SSB) and

*Corresponding author. E-mail: mohsaltab@yahoo.com.

tandem single-sideband (TSSB), have been widely used. Both SSB and TSSB SCMs can be obtained using optical Mach-Zehnder modulators (Seed and Williams, 2007; Azizur et al., 2006; Wu and Chang, 2006).

In mm-wave fiber-radio systems, electrooptic intensity modulators [e.g., a dual electrode Mach–Zehnder modulator (DE-MZM)], suitable for generating OSSB+C modulation, often exhibit reduced optical modulation depths (carrier-to-sideband ratios, CSRs >10 dB are typical) which leads to poor overall link performances. This situation can be improved by employing techniques where the CSRs of the modulated channels are reduced by some external means. However, such schemes often require additional wavelength-selective components, which are inherently susceptible to performance degradation. If the multifunctional WDM optical interface, however, can be modified in such a way that the CSRs are reduced by avoiding additional hardware and while still retaining its usual functionality, an efficient and effective fiber-radio network architecture can be achieved (Rubio et al., 2005; Yu et al., 2007; Bakaul et al., 2007, 2006).

Potassium Dihydrogen Phosphate (KDP) and Potassium Dideuterium Phosphate (DKDP) are currently used for electro-optical modulation and frequency conversion. CORETECH's KDP and DKDP have high nonlinear coefficient and high optical damage threshold, and can be used for electro-optical modulator, Q switches and shutters for high speed photography (Website: www.coretech.com.cn or www.soullon.com).

In the presented paper, the design of electrooptic modulator that applied in radio–over–fiber (ROF) application will be designed and investigated with a designed tank circuit to maximize the output power. The nonlinear distortion has been analyzed also.

BASIC MODEL, GOVERNING EQUATIONS, AND ANALYSIS

The ratio of the output intensity to the input in crystal modulator is given by:

$$\frac{I_o}{I_i} = \sin^2\frac{\Gamma}{2} = \sin^2\left[\left(\frac{\pi}{2}\right)\frac{V}{V_\pi}\right] \quad (1)$$

The transmission factor (I_o/I_i) is plotted in Figure 1 against the applied voltage, where the process of amplitude modulation of an optical signal is illustrated. The modulator is usually biased with fixed retardation, Γ_B = π/2 to the 50% intensity transmission point. A small applied sinusoidal voltage modulates the transmitted intensity about the bias point.

To treat the situation depicted by Figure 1 mathematically, one can take:

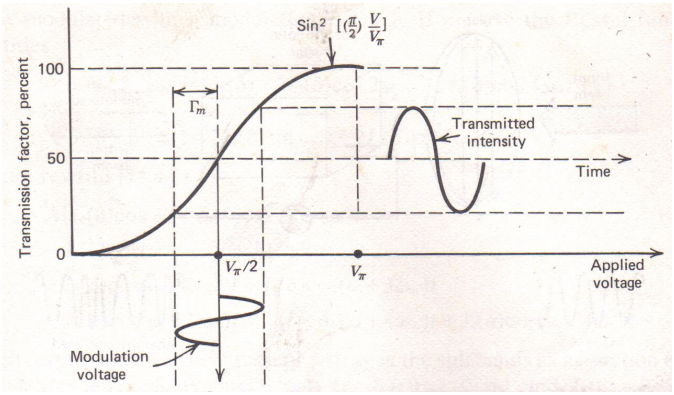

Figure 1. Transmission factor of a cross-polarized electro-optic modulator as a function of an applied voltage. The modulator is biased to the point $\Gamma_B = \pi/2$, which results in a 50% intensity transmission.

$$\Gamma = \frac{\pi}{2} + \Gamma_m \sin\omega_m t \quad (2)$$

Where the retardation bias is taken as π/2, and Γ_m is related to the amplitude V_m of the modulation voltage $V_m \sin \omega_m t$; thus $\Gamma_m = \pi (V_m/V_\pi)$.

Using Equation (2) into Equation (1) one can obtain:

$$\frac{I_o}{I_i} = \sin^2\left(\frac{\pi}{4} + \frac{\Gamma_m}{2}\sin\omega_m t\right) \quad (3)$$

$$= \frac{1}{2}\left[1 + \sin\left(\Gamma_m \sin\omega_m t\right)\right] \quad (4)$$

That, for $\Gamma_m << 1$, becomes:

$$\frac{I_o}{I_i} \cong \frac{1}{2}\left(1 + \Gamma_m \sin\omega_m t\right) \quad (5)$$

So that the intensity modulation is a linear replica of the modulating voltage $V_m \sin \omega_m t$. If the condition $\Gamma_m << 1$ is not fulfilled, it follows from Figure 1 or from Equation (4) that the intensity variation is distorted and will contain an appreciable amount of higher odd harmonics.

For the maximum output power, the electro - optic crystal is placed between two electrodes with modulation field containing frequencies near the resonance one, $\omega_o/2\pi$ applied to it. R_s is the internal resistance of the modulation source and C represents the parallel-plate capacitance due to electro - optic crystal, where; $\omega_o^2 = (LC)^{-1}$, as shown in Figure 2. Therefore, the maximum modulation bandwidth (the frequency spectrum occupied by the modulation signal) must be less than (with R_L=R_S)

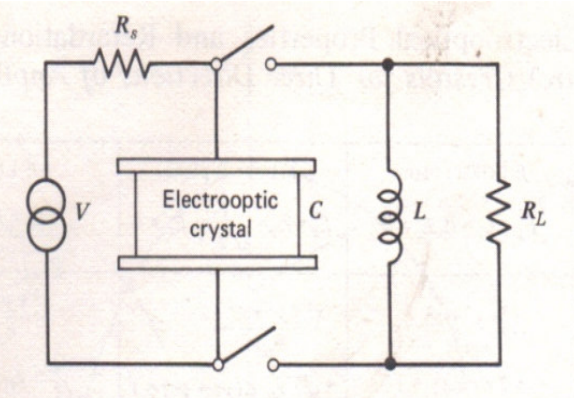

Figure 2. Equivalent circuit of an electro-optic modulation crystal in a parallel plate configuration.

$$\frac{\Delta\omega}{2\pi} = \frac{1}{2\pi R_L C} \tag{6}$$

Using the peak modulation voltage $V_m = (E_z)_m\, l$, one can show, with the aid of Eqn.(6), that the power $V_m^2 / 2R_L$ needed in KDP- type crystals to obtain a peak retardation Γ_m is related to the modulation bandwidth $\Delta v = \Delta\omega / 2\pi$ as:

$$P = \frac{\Gamma_m^2 \lambda^2 A \varepsilon \Delta v}{4\pi l\, n_o^6\, r_{63}^2} \text{, Watt} \tag{7}$$

Where l is the length of the optical path in the crystal, A is the cross sectional area of the crystal normal to l, and $\varepsilon = \varepsilon_o \cdot \varepsilon_r$ is the dielectric constant at the modulation frequency ω_o.

The electro-optic retardation due to a field E can be written as:

$$\Gamma = a\, E\, l \tag{8}$$

Where; $a = \omega n_o^3\, r_{63} / c$.

The highest useful modulation frequency is found to be for a KDP crystal (Website: www.coretech.com.cn or www.soullon.com)

$$(v_m)_{\max} = \frac{c}{4ln} \tag{9}$$

The impact of nonlinear distortion in radio over fiber systems with single-sideband and tandem single-sideband sub carrier modulations (Yariv, 1991) is processed based on Eqn. (3), where we have:

$$\frac{I_o}{I_i} = \sin^2\left(\frac{\Gamma}{2}\right) \text{ With}$$

$$\Gamma = \frac{\pi}{2} + \phi_D + \Gamma_m \sin\omega_m t \tag{10}$$

Where; ϕ_D is the deviation angle.

The use of Equation (10) into Equation (3) yields

$$\frac{I_o}{I_i} = \sin^2\left(\frac{\pi}{4} + \frac{\phi_D}{2} + \frac{\Gamma_m}{2}\sin\omega_m t\right) = \frac{1}{2}\left[1 + \sin\left(\phi_m + \phi_{D_o}\right)\right]$$

Where; $\phi_m = \Gamma_m \sin\omega_m t$ <<1. Thus, we have:

$$\frac{I_o}{I_i} = \frac{1}{2}\left[1 + \sin\varphi_m \cos\phi_D + \cos\phi_m \sin\phi_D\right]$$

Thus

$$\frac{\Delta I_o}{I_i} = \frac{1}{2}\Gamma_m \cos\phi_D \sin\omega_m t + \frac{1}{2}\sin\phi_D \tag{11}$$

Equation 11 indicates that the variation of the output of the modulators has two components:

Permanent distortion component,

$$PDC = \frac{1}{2}\sin\phi_D \tag{12}$$

Modulated-amplitude component,

$$MAC = \frac{1}{2}\Gamma_m \cos\phi_D \sin\omega_m t \tag{13}$$

Where; R_D = PDC/MAC is the ratio of the two components.

In the present paper, two tasks will be done:

The design of the tank circuit to maximize the output power. The variation of the R_D against the deviation angle ϕ_D

Where:

$$-\frac{\pi}{3} \le \phi_D \le \frac{\pi}{3} .$$

ANALYSIS

Both the input power P_i and the output power P_o of the modulator are given by:

$$P_i = \frac{V_m^2}{2R_L} \quad (14)$$

$$P_o = \frac{\Gamma_m^2 \lambda^2 A \varepsilon \Delta v}{4\pi l n_o^6 r_{63}^2} \quad (15)$$

Where; the resonance frequency ω_r and the bandwidth Δω are:

$$\omega_r^2 = \frac{1}{LC} - \frac{L^2}{r^2} \quad (16)$$

$$\Delta\omega = \frac{1}{RC} \quad (17)$$

Also, we have:

$$\Gamma_m = \frac{\pi V_m}{V_\pi} \quad (18)$$

$$(\omega_r)_{\max} = \frac{c}{4ln} = \frac{0.75x10^8}{ln} \quad (19)$$

$$V_\pi = \frac{\lambda}{2n_o^3 r_{63}} \quad (20)$$

Assuming that A = l^2, the modulator efficiency is given by:

$$\eta = \frac{P_i}{P_o} = l\ \varepsilon\ \Delta\omega R n_o^6, \quad \frac{\eta C}{l} = \varepsilon_o n_o^6 \quad (21)$$

Thus η is proportional to *l* and inversely proportional to C. To design at maximum efficiency i.e., η =1, we must make:

$$C = \varepsilon_o n_o^6 l \quad (22)$$

To work at certain ω_o , we must make:

$$L = \frac{1}{\omega_o^2 C} \quad (23)$$

To work at given bandwidth $\Delta\omega$, we must have:

$$R = \frac{1}{\Delta\omega C} \quad (24)$$

Or

$$\frac{R}{L} = \frac{\omega_o^2}{\Delta\omega} \quad (25)$$

In general, if $\eta \neq 1$, we have:

$$C = \frac{\varepsilon_o n_o^6 l}{\eta}, \quad (26)$$

$$L = \frac{1}{\omega_o^2 C} = \frac{\eta}{\varepsilon_o n_o^6 l \omega_o^2}, \text{ and} \quad (27)$$

$$R = \frac{1}{\Delta\omega C} \text{ or } \frac{R}{L} = \frac{\omega_o^2}{\Delta\omega} \quad (28)$$

We will treat the design of the tank circuit at the following set of parameters:

$$70\% < \eta < 95\%$$

$$2\pi x10 \le \omega_o, \frac{GRad}{\sec} \le 2\pi x40$$

$$2\pi x1 \le \Delta\omega, \frac{GRad}{\sec} \le 2\pi x4$$

RESULTS AND DISCUSSIONS

The following are the physical parameters of KDP modulator crystal (Yariv, 1991) and the numerical ranges that employed in the present paper are: n_o is the refractive index = 1.4968, λ is the optical wavelength = 0.546 *μm*, r_{63} is the electro-optic coefficient = 10.3 x 10^{-12} *m/V*,*l* is the crystal length 0.2 <*l* cm< 1.0, A is the crystal cross-section area = l^2, R_L is the load resistor, C is the load capacitor, L is the load inductance.

Special software is designed to process two items of special emphases that is, the ratio R_D the parametrical design of the tank circuit {R_L, L, C}.

Thus, we have four effects {R_D, R_L, L, C}, and five causes {ϕ_D , *l*, ω_r, $\Delta\omega$, η}.

Variations of R_D against variations of the deviation angle are displayed in Figure 3, at different Γ_m we get: {R_D and ϕ_D} are in negative strong correlation while {R_D and Γ_m} are in positive strong correlation.

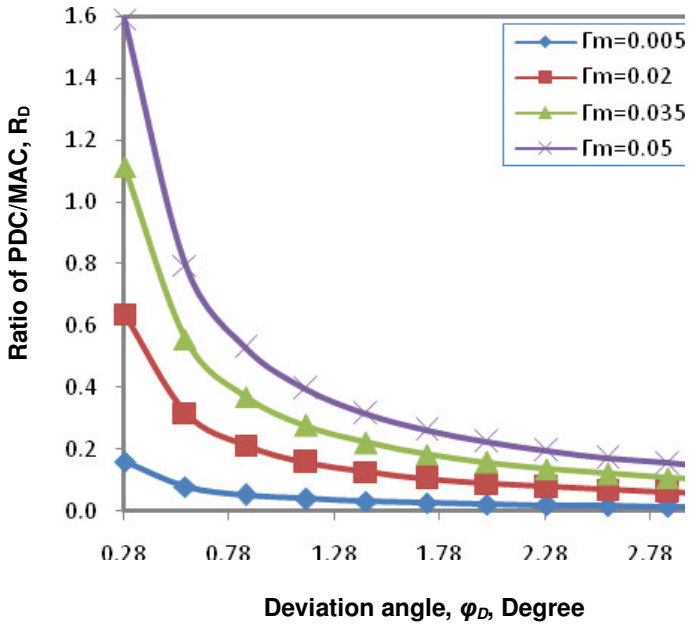

Figure 3. Variation of R_D against variations of the deviation angle φ_D.

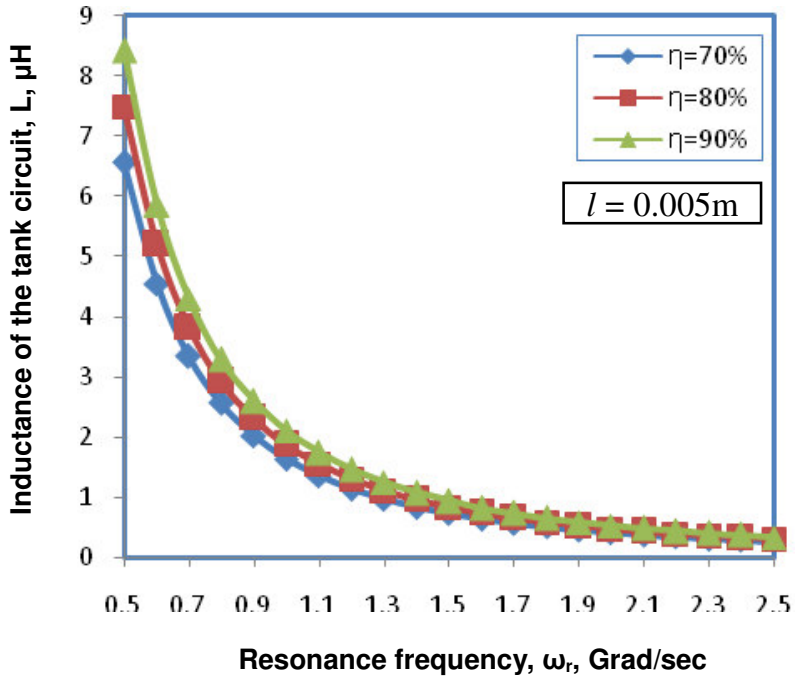

Figure 4. Variation of inductance of tank circuit, L, against variations of the resonance frequency, ω_r at the assumed set of parameters

Variations of the tank circuit inductance, L. against variations of one or more of {ω_r, η, *l*} are displayed in Figures 4 - 8, where the following are assured:

1) The increase of the microwave resonance frequency ω_r reduces the inductance L.
2) The increase of the modulator length, *l*, reduces the.

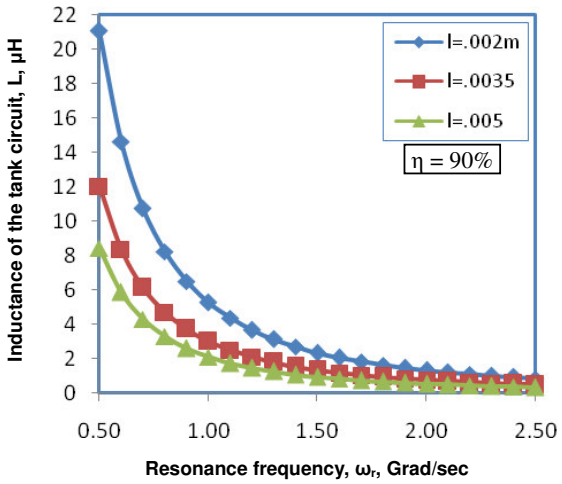

Figure 5. Variation of inductance of tank circuit, L, against variations of the resonance frequency, ω_r, at the assumed set of parameters.

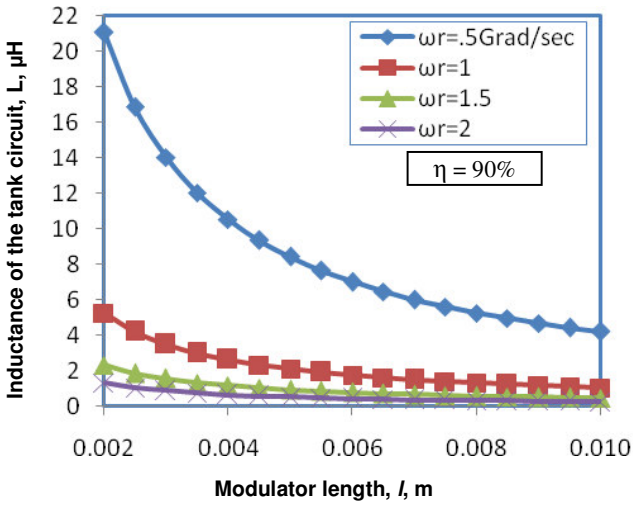

Figure 6. Variation of inductance of tank circuit, L, against variations of the modulator length, l, at the assumed set of parameters.

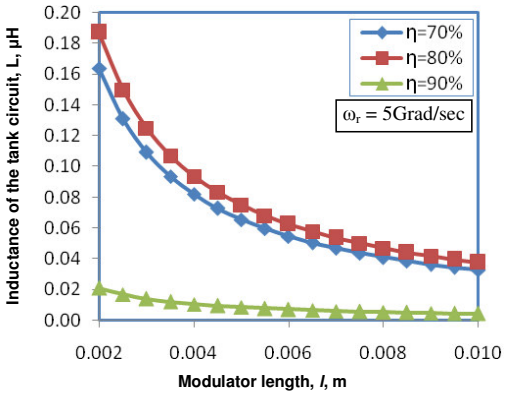

Figure 7. Variation of inductance of tank circuit, L, against variations of the modulator length, l, at the assumed set of parameters.

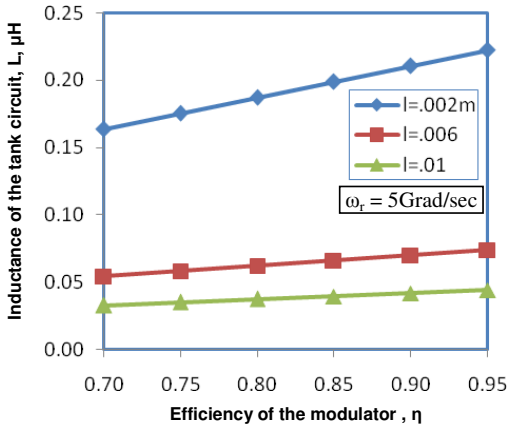

Figure 8. Variation of inductance of tank circuit, L, against variations of the efficiency of the modulator, η, at the assumed set of parameters

inductance L
3.) Finally to increase the efficiency η, we must reduce L.

Variations of the tank circuit capacitance, C, against variations of one or more of {*l*, η} is clarified in Figures 9 and 10, where the following are found:

1.) C and *l* are in strong positive correlations.
2.) For higher values of η, C must be reduced.

Variations of the tank circuit resistance, R_L, against variations of one or more of {$\Delta\omega$, *l*, η} are displayed in

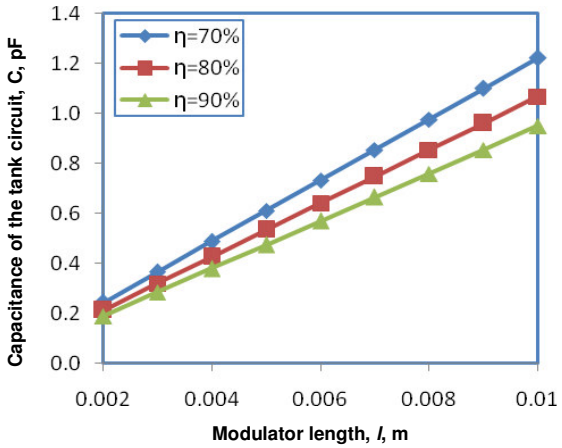

Figure 9. Variation of capacitance of tank circuit, C, against variations of the modulator length, l, at the assumed set of parameters.

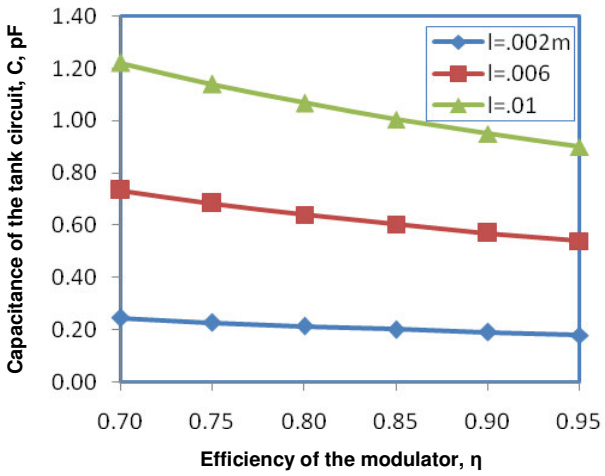

Figure 10. Variation of capacitance of tank circuit, C, against variations of the efficiency of the modulator, η, at the assumed set of parameters.

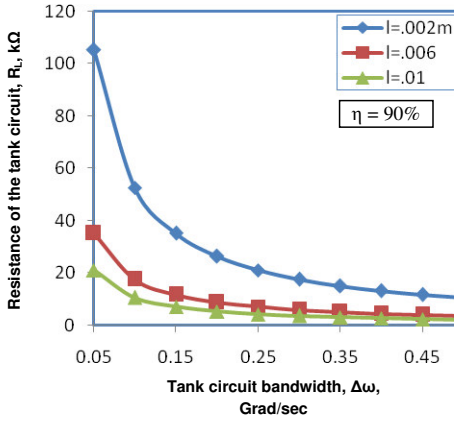

Figure 11. Variation of resistance of tank circuit, RL, against variations of the tank circuit bandwidth, Δω, at the assumed set of parameters.

Figures 11 - 16, where the following are clarified:

1.) R_L is in strong negative correlations with $\Delta\omega$ or *l* or both.
2.) R_L and η are in linear positive correlation.

Conclusion

In the present paper, we have modeled and parame-rically investigate the performance of the tank circuit used with electro-optic modulator made of KDP crystal and operate in the microwave range. The parameters of the modulator (R_L, L and C) are investigated under wide ranges of the set of causes ($^{\Delta}\omega$, ω_r, *l*, η). The effect of

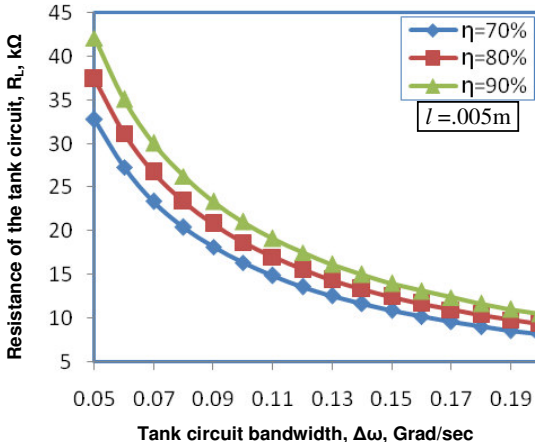

Figure 12. Variation of resistance of tank circuit, R_L, against variations of the tank circuit bandwidth, Δω, at the assumed set of parameters

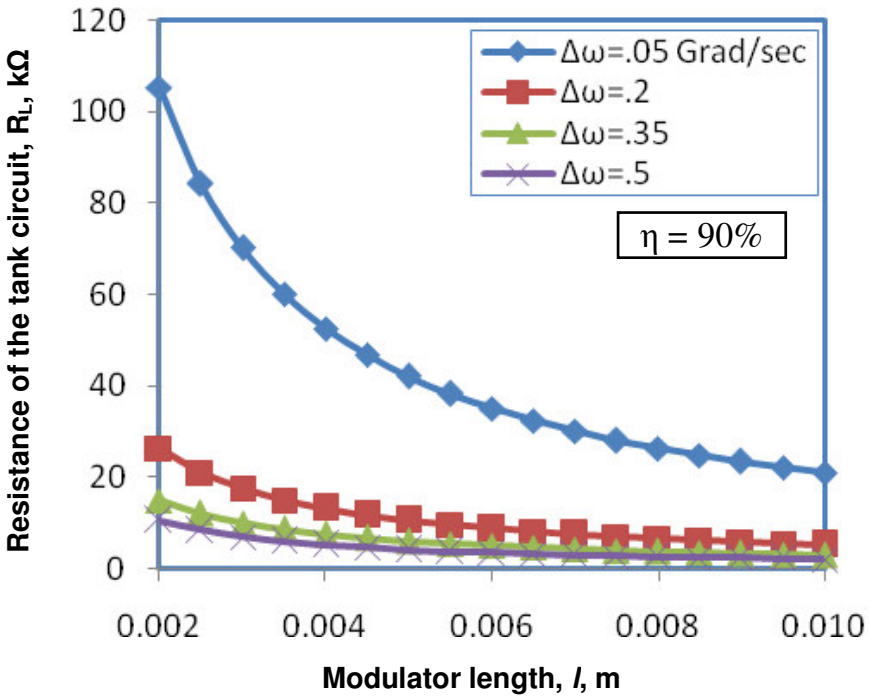

Figure 13. Variation of resistance of tank circuit, RL, against variations of the modulator length, l, at the assumed set of parameters.

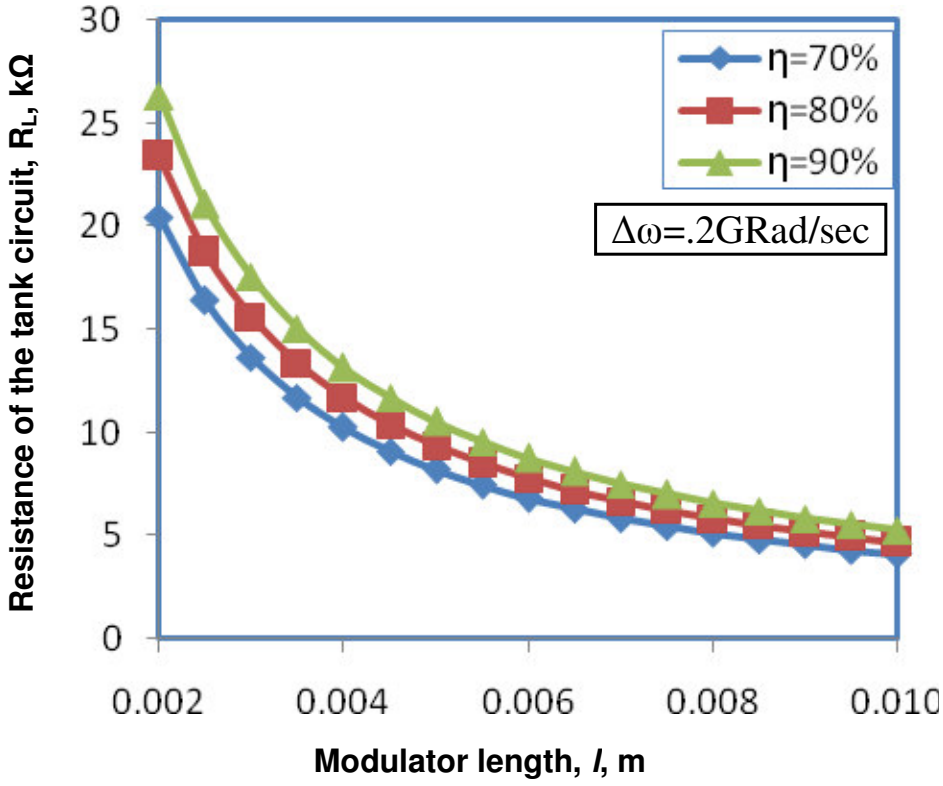

Figure 14. Variation of resistance of tank circuit, RL, against variations of the modulator length, l, at the assumed set of parameters.

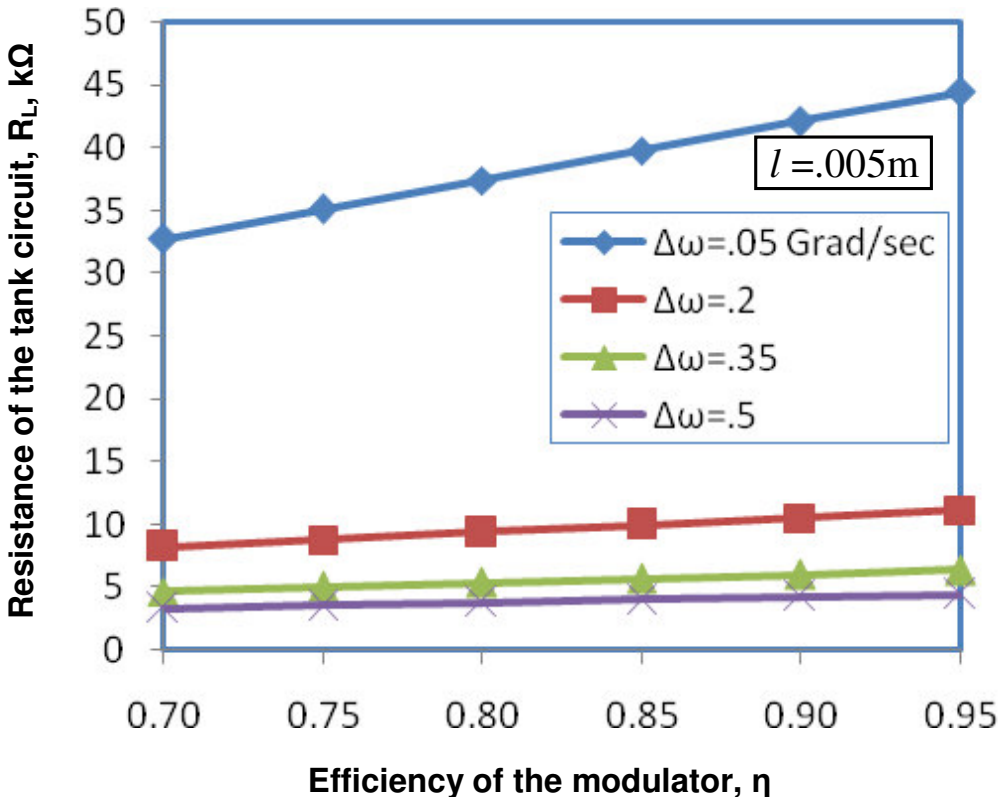

Figure 15. Variation of resistance of tank circuit, RL, against variations of the efficiency of the modulator, η, at the assumed set of parameters.

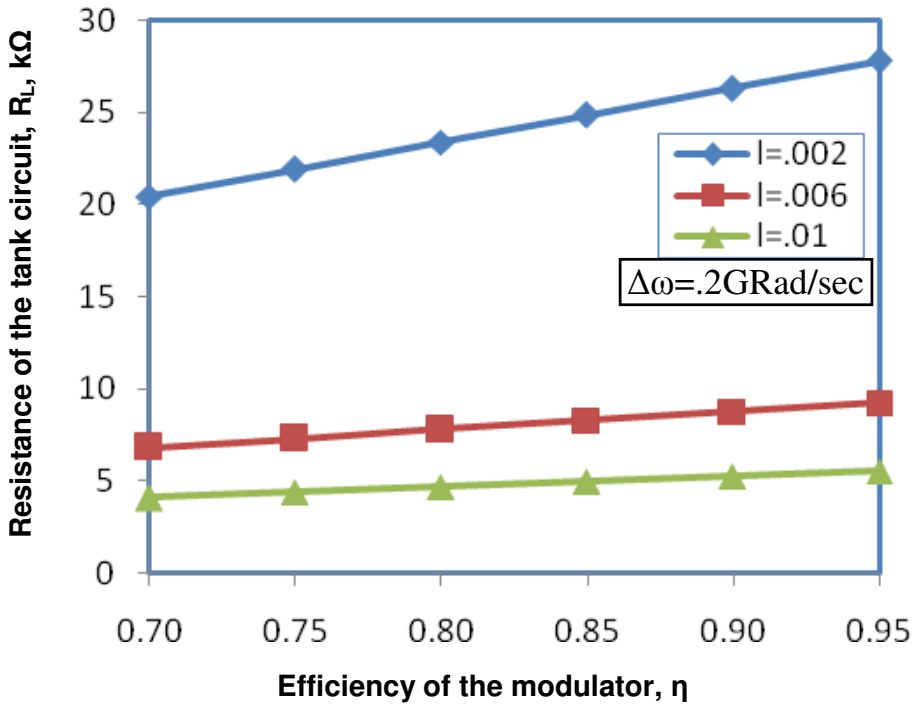

Figure 16. Variation of resistance of tank circuit, RL, against variations of the efficiency of the modulator, η, at the assumed set of parameters.

effect of deviation of the biasing voltage is also investigated where severe reduction effects are assured.

REFERENCES

Azizur RBM, Haxha V, Haxha S, Grattan KTV (2006). "Design Optimization of Polymer Electrooptic Modulators," J. Lightwave Technol. 24(9): 3506-3513.

Bakaul M, Nirmalathas A, Lim C, Novak D (2007). Waterhouse R, "Investigation of Performance Enhancement of WDM Optical Interfaces for Millimeter-Wave Fiber-Radio Networks," IEEE Photonic Technol. Lett. 19(11): 843-845.

Bakaul M, Nirmalathas A, Lim C, Novak D (2006). Waterhouse R, "Experimental Characterization of Single and Cascaded WDM Optical Interface in a MM-Wave Fiber-Radio Network," IEEE Phtonics Technol. Lett. 18(1): 115-117.

Chang YD, Choi KS, Sim JS, Yu HK, Kim J (2007). "A 60-GHz-Band Analog Optical System-on-Package Transmitter for Fiber-Radio Communications," J. Lightwave Technol. 25(11): 1-6.

Chul H, Kim H, Chur Y (2009). "Full-Duplex Radio-Over-Fiber System Using Phase-Modulated Downlink and Intensity-Modulated Uplink", IEEE Photonic Technol. Lett. Pirelli Broadband Solution, "Radio Over Fiber (ROF)", Photonics@pirelli.com, Milano, Italy, 2006. 21(1): 9-11

Kim HB, Woesner H, Wolisz A (2003). "A Medium Access Control Protocol for Radio Over Fiber Wireless LAN Operating in the 60-GHz Band," 5th European Personal Mobile Comm. Conf. (EPMCC).

Rubio DS, Keil UD, Liao L, Franck T, Liu A, Hodge D W, Rubin D, Cohen R (2005). "Customized Drive Electronics to Extend Silicon Optical Modulators to 4 Gb/s," J. Lightwave Technol. 23(12): 4305-4314.

Seed AJ, Williams KJ (2007). "Performance of Optical OFDM in Ultralong-Haul WDM Lightwave Systems," J. Lightwave Technol. 25(1): 131-138.

Wu C, Chang X (2006). "Impact on Nonlinear Distortion in Radio Over Fiber Systems With Single-Sideband and Tandem Single-Sideband Subcarrier Modulations," J. Lightwave Technol. 24(5): 2076-2090.

Yariv A (1991). Optical Electronics, Holt Rinehart and Winston, U. S. A, 4th ed.

Yu J, Jia Z, Wang T, Chang GK (2007). "Centralized Lightwave Radio-Over-Fiber System With Photonic Frequency Quadrupling for High-Frequency Millimeter-Wave Generation," IEEE Photonic Technol. Lett. 19(19): 1499-1501.